Contribution from the School of Chemical Sciences,
University of Illinois, Urbana, Illinois 61801

^{17}O Nuclear Magnetic Resonance Spectroscopy of Polyoxometalates. 2. Heteronuclear Decoupling of Quadrupolar Nuclei

C. J. BESECKER, W. G. KLEMPERER,* D. J. MALTBIE, and D. A. WRIGHT

Received June 7, 1984

The influence of ^{51}V, ^{93}Nb, ^{181}Ta, ^{95}Mo, ^{97}Mo, and ^{183}W spin–spin coupling on ^{17}O solution NMR spectral resolution is examined, and only ^{51}V and ^{93}Nb coupling is found to affect ^{17}O NMR line widths substantially. Double-resonance $^{17}O\{^{93}Nb\}$ studies of the $NbW_5O_{19}^{3-}$ and $Nb_2W_4O_{19}^{4-}$ anions show how metal decoupling can reduce ^{17}O NMR line widths by factors up to $^1/_{30}$. Selective metal decoupling is also shown to be a powerful technique in an $^{17}O\{^{51}V\}$ study of aqueous $Na_6V_{10}O_{28}$ solutions containing both decavanadate $V_{10}O_{28}^{6-}$ and metavanadate $(VO_3)_n^{n-}$ ions. Selective decoupling experiments yield unambiguous structural assignments for all resonances in the fully resolved ^{17}O and ^{51}V decavanadate NMR spectra. Decoupling of the metavanadate ^{51}V resonances at two different temperatures allows chemical-exchange effects to be separated from competing thermal-decoupling and quadrupolar-broadening effects, leading to the discovery of a previously hidden dynamic process involving metavanadate ions.

In the first part of this series,[1] an attempt was made to delineate the scope and limitations of ^{17}O solution NMR spectroscopy as a structural and dynamic probe in early-transition-metal polyoxoanion chemistry. Since the ability to derive structural and dynamic information from ^{17}O NMR spectra depends critically upon high spectral resolution, attention was focused principally on methods for obtaining narrow line widths by reducing the quadrupolar relaxation rate of the spin $^5/_2$ ^{17}O nucleus. In many cases, however, ^{17}O NMR line widths are not controlled by ^{17}O quadrupolar relaxation but instead by spin–spin coupling to other quadrupolar nuclei. The spectrum of the $[(C_5(CH_3)_5)Rh(cis\text{-}Nb_2W_4O_{19})]^{2-}$ anion as a mixture of three diastereomers, shown in Figure 1, is illustrative.[2] Here, narrow ^{17}O NMR line widths are observed for oxygens bonded only to spin $^1/_2$ or spin 0 rhodium and/or tungsten nuclei. Regions of the spectrum containing resonances assigned to oxygens bonded to one or more quadrupolar, spin $^9/_2$ ^{93}Nb nuclei are unresolved, however, and contain only broad, relatively featureless resonances. The complications introduced by coupling to quadrupolar nuclei extend beyond resolution problems. Dynamic effects, for example, can be obscured by metal–oxygen spin–spin coupling since chemical exchange in the slow-exchange domain and thermal decoupling[3] can both produce line narrowing as the temperature is lowered.

This paper addresses several questions concerning spin–spin coupling between the ^{17}O nucleus and early-transition-metal nuclei in polyoxoanions. First, the influence of ^{51}V, ^{93}Nb, ^{181}Ta, ^{95}Mo, ^{97}Mo, and ^{183}W coupling on ^{17}O NMR line widths is examined, and the effectiveness of thermal decoupling is assessed. Then three double-resonance decoupling studies are described: $^{17}O\{^{93}Nb\}$ NMR studies of $NbW_5O_{19}^{3-}$ and $Nb_2W_4O_{19}^{4-}$ and an $^{17}O\{^{51}V\}$ NMR study of aqueous $Na_6V_{10}O_{28}$ solutions containing both $V_{10}O_{28}^{6-}$ and $(VO_3)_n^{n-}$ ions.

Experimental Section

A. NMR Spectral Measurements. ^{17}O, ^{93}Nb, and ^{51}V spectra were measured on an unlocked FTNMR system with a 5.87-T Oxford Instruments magnet and a Nicolet NIC-80 data system. The probe was designed to give maximum decoupling with minimum power. A nonstandard two-coil configuration was employed in which the inner coil was used for decoupling as well as observing vanadium and niobium and the outer coil was used for observing oxygen. Both coils were of the Helmholtz type and were constructed from 18-gauge wire. The observed coil dimensions were 30-mm height and 29-mm diameter; the decoupling coil dimensions were 25-mm height and 15-mm diameter. High-voltage (5-kV) capacitors were used on both channels. The amount of sample used for each measurement was sufficient to fill a 12 mm o.d. vertical NMR tube to a height of 30 mm (ca. 2.6 mL solution volume). The instrumental setup involved a standard $^1/_4$-wave protection scheme on the receiver channel, with a band-pass filter on the decoupling channel and a low-pass filter on the observe channel.

Oxygen-17 NMR spectra were ^{51}V and ^{93}Nb decoupled with use of continuous-wave single-frequency radiation, which was applied to samples only during data acquisition. Decoupling power levels of 1.5, 10, and 22 W were used to decouple polyvanadate, $NbW_5O_{19}^{3-}$, and $Nb_2W_4O_{19}^{4-}$ spectra, respectively. A 50% duty cycle was used to reduce sample heating. In the absence of cooling gas, the decoupler typically heated the sample 8–12 °C when decoupling at 22 W. The sample temperature was monitored during data collection with a thermocouple built into the probe to measure cooling-gas temperature. This thermocouple was calibrated before each run by placing another thermocouple in a 12-mm sample tube in the solvent being used in the sample, lowering this assembly into the probe, and then equilibrating the thermocouple with use of a standard variable-temperature apparatus while the decoupler was in operation. The magnet was shimmed by tuning the observe coil to cesium and observing an aqueous CsI sample.

All spectra were obtained with use of cylindrical 12 mm o.d. vertical sample tubes without sample spinning and were referenced externally to the appropriate standard with use of the sample replacement method. Chemical shifts for all nuclei are reported as positive numbers for resonances that are observed at higher frequency (lower field) than the reference used. All reported line widths have been corrected for exponential line broadening. The following abbreviations are used when listing spectral parameters: sol for solvent, |x| for molar concentration of x, T for temperature in °C, enr for ^{17}O content in atom percent, np for number of pulses, exp for exponential line broadening in hertz, sf for spectrometer frequency in megahertz, pw for the observe pulse width in μs, and de for the preacquisition delay time in μs.

^{17}O NMR. Oxygen-17 NMR chemical shifts were referenced to 25 °C fresh tap water. The pulse repetition rate was 2.94 Hz during double-resonance experiments but 5.88 Hz otherwise. A spectral bandwidth of 50 000 Hz was digitized with use of 8192 data points. The error limits associated with ^{17}O chemical shift values are ±3 ppm for line widths <200 Hz, ±5 ppm for line widths >200 but <400 Hz, and ±7 ppm for line widths >400 Hz. The error limits associated with line width values are ±20 Hz for line widths <100 Hz, ±40 Hz for line widths >100 but <400 Hz, and ±15% for line widths >400 Hz. Experimental parameters for ^{17}O NMR measurements are listed below.

$TaW_5O_{19}[(n\text{-}C_4H_9)_4N]_3$: sol = CH_3CN, |Ta| = 0.011, enr = 20, exp = 5, sf = 33.923, pw = 35, de = 20, np = 4000.

$NbW_5O_{19}[(n\text{-}C_4H_9)_4N]_3$: sol = CH_3CN, |Nb| = 0.011, enr = 20, exp = 5, sf = 33.923, pw = 35, de = 20. For T = 28, np = 4000; for all other temperatures np = 8000.

$Nb_2W_4O_{19}[(n\text{-}C_4H_9)_4N]_4$: sol = CH_3CN, |Nb| = 0.082, enr = 20, exp = 5, sf = 33.923, pw = 33, de = 20, np = 2000.

Aqueous $Na_6V_{10}O_{28}$: sol = H_2O, |V| = 1.8, enr = 2, exp = 5, sf = 33.935, pw = 16, de = 24. For T = 44, np = 5000; for T = 19, np = 6000.

^{93}Nb NMR. Niobium-93 NMR chemical shifts were referenced to a 0.25 M solution of $NbCl_6[(C_2H_5)_4N]$ in CH_3CN. The pulse repetition rate was 12.1 Hz; a spectral bandwidth of 50 000 Hz was digitized with use of 4096 data points. The error limits associated with ^{93}Nb chemical shift values are ±5 ppm for line widths >500 but <1000 Hz and ±10 ppm for line widths >1000 Hz. The error limits associated with line

(1) Filowitz, M.; Ho, R. K. C.; Klemperer, W. G.; Shum, W. *Inorg. Chem.* **1979**, *18*, 93–103.
(2) Besecker, C. J.; Day, V. W.; Klemperer, W. G.; Thompson, M. R. *J. Am. Chem. Soc.* **1984**, *106*, 4125–4136.
(3) (a) Roberts, J. D. *J. Am. Chem. Soc.* **1956**, *78*, 4495–4496. (b) Muetterties, E. L.; Phillips, W. D. *J. Am. Chem. Soc.* **1959**, *81*, 1084–1088. (c) Beall, H.; Bushweller, C. H.; Dewkett, W. J.; Grace, M. *J. Am. Chem. Soc.* **1970**, *92*, 3484–3486.

0020-1669/85/1324-1027$01.50/0

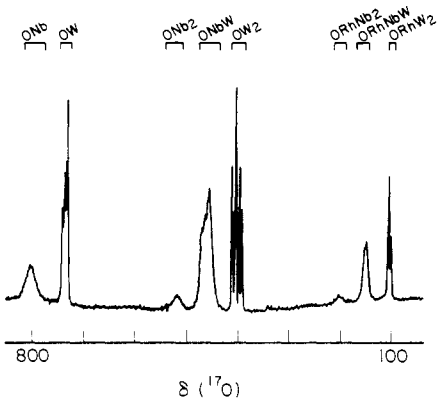

Figure 1. 33.9-MHz ^{17}O NMR spectrum of $[((CH_3)_5C_5)Rh(cis\text{-}Nb_2W_4O_{19})][(n\text{-}C_4H_9)_4N]_2$ in CH_3CN as a three-diastereomer mixture. Only the δ 50–850 region is shown. See ref 2 for structural and spectral data. The assignments given indicate the identity and number of metal(s) each type of oxygen is bonded to; e.g., an $ORhW_2$ oxygen is bonded to one rhodium and two tungsten atoms.

width values are ±15% for line widths >500 Hz but <1000 Hz and ±20% for line widths >1000 Hz. Experimental parameters for ^{93}Nb measurements are listed below.

$NbW_5O_{19}[(n\text{-}C_4H_9)_4N]_3$: sol = CH_3CN, |Nb| = 0.011, enr = 20, exp = 10, sf = 61.175, pw = 28, de = 20, np = 2000.

$Nb_2W_4O_{19}[(n\text{-}C_4H_9)_4N]_4$: sol = CH_3CN, |Nb| = 0.082, enr = 20, exp = 40, sf = 61.172, pw = 28, de = 20, np = 2000.

^{51}V NMR. Vanadium-51 chemical shifts were referenced to a 25 °C sample of neat $VOCl_3$ (Aldrich). The pulse repetition rate was 5.88 Hz; a spectral bandwidth of 50 000 Hz was digitized with use of 8192 data points. The error limits associated with ^{51}V chemical shifts and line widths are the same as those given for ^{17}O NMR spectra. Experimental parameters for aqueous $Na_6V_{10}O_{28}$ ^{51}V NMR measurements were as follows: sol = H_2O, |V| = 1.8, enr = 2, exp = 0.0, sf = 65.78, pw = 16, de = 50. For T = 44 and 35, np = 5000; for T = 19, np = 10 000.

B. Sample Preparation. Reagents, Solvents, and General Procedures. The following were purchased from commercial sources and used without further purification: $Na_2WO_4{\cdot}2H_2O$ and glacial acetic acid (Fisher); 30% aqueous H_2O_2, 85% hydrated KOH pellets and sulfuric acid (Mallinckrodt); Nb_2O_5 and $(n\text{-}C_4H_9)_4NBr$ (Aldrich); $(CH_3)_4NBr$ and 0.4 M aqueous $(n\text{-}C_4H_9)_4NOH$ (Eastman); $Nb(OC_2H_5)_5$ and $Ta(OC_2H_5)_5$ (Alfa); 50–100 mesh sulfonated 2% cross-linked polystyrene cation-exchange resin in hydrogen form (Bio-Rad); $Na_2S_2O_4{\cdot}2H_2O$ (Amend); ^{17}O-enriched water (Monsanto Research).

$K_7HNb_6O_{19}{\cdot}13H_2O$ was prepared according to literature procedures.[1,4] Experience showed that the product could be obtained reproducibly as well-formed crystals only if deionized water was employed and this water was degassed by boiling vigorously for 15 min immediately before use. Oxygen-17-enriched $(Nb_2W_4O_{19})[(n\text{-}C_4H_9)_4N]_4$ was prepared as described in ref 2. $Na_6(V_{10}O_{28}){\cdot}18H_2O$ was prepared with use of a method reported by Murmann and Johnson.[5] $WO_4[(n\text{-}C_4H_9)_4N]_2$ was synthesized according to the procedure in ref 6.

Anhydrous diethyl ether (Mallinckrodt) was used only from freshly opened cans. $Cl_3C_2O_2H$ (Fisher) was ground with a mortar and pestle and dried under vacuum before use. Acetonitrile (Aldrich, 99%) was stored over activated 3-Å sieves. Chloroform and 1,2-dichloroethane (Fisher) were stored over activated 4-Å molecular sieves (Linde). Solvents used for the preparation of ^{17}O-enriched samples were purified more thoroughly before use. Ethanol (U.S. Industrial Chemical Co.) was dried with magnesium ethoxide according to a literature procedure.[7] Acetonitrile was distilled under N_2 from P_4O_{10} onto activated 3-Å molecular sieves (Linde). Chloroform was distilled under N_2 from P_4O_{10} onto activated 3-Å molecular sieves. Molecular sieves were activated by drying at 350 °C for 24 h and storing under N_2 at room temperature.

All manipulations of ^{17}O-enriched WO_4^{2-}, $NbW_5O_{19}^{3-}$, and $Nb_2W_4O_{19}^{4-}$ salts were performed in closed systems with vigorous exclusion of atmospheric moisture to avoid isotopic dilution.

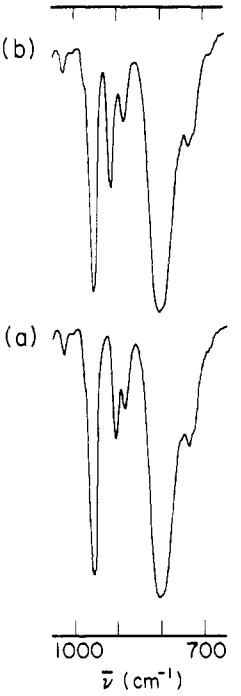

Figure 2. IR spectra of (a) $(TaW_5O_{19})[(n\text{-}C_4H_9)_4N]_3$ and (b) $(NbW_5O_{19})[(n\text{-}C_4H_9)_4N]_3$ measured from Nujol mulls. See Experimental Section for numerical data.

Analytical Procedures. Elemental analyses were performed by the School of Chemical Sciences analytical laboratory and by Galbraith Laboratories, Knoxville, TN. Infrared spectra were measured from mineral oil (Nujol) mulls between NaCl plates on a Perkin-Elmer 1330 spectrometer and were referenced to the 1028-cm^{-1} band of a 0.05-mm polystyrene film.

$TaW_5O_{19}[(n\text{-}C_4H_9)_4N]_3$.[8] A 10.0-g (13.7-mmol) sample of $WO_4[(n\text{-}C_4H_9)_4N]_2$ was enriched in ^{17}O by stirring for 1 h in 6.0 mL of ^{17}O-enriched water. The resulting solution was freeze–thaw degassed four times, the solution was frozen, and the water was recovered by vacuum sublimation at room temperature into a receiving flask maintained at liquid-nitrogen temperature. The resulting solid was dried overnight under vacuum at 50 °C. The enriched $WO_4[(n\text{-}C_4H_9)_4N]_2$ was then dissolved into 10 mL of CH_3CN. A second solution containing 2.78 g (6.85 mmol) of $Ta(OC_2H_5)_5$ and 2.24 g (13.7 mmol) of $Cl_3C_2O_2H$ in 5 mL of CH_3CN was stirred for ca. 1 min to obtain a homogeneous solution. This solution was then added dropwise over 2 min to the enriched $WO_4[(n\text{-}C_4H_9)_4N]_2$ solution with rapid stirring. The resulting solution heated up, bubbled, and turned yellow; rapid stirring was continued for ca. 30 min. During this time a white solid precipitated. Addition of ca. 150 mL of ether completed precipitation of the white product, which was suction filtered and washed with ca. 25 mL of ether to yield ca. 5 g of white powder. (In some cases, if solvents were insufficiently dry, the product precipitated as an oil. When this occurred, the supernatant liquid was decanted and the oil was stirred with 5–6 mL of ethanol for 2 min. Ether was then added to precipitate the product as a white powder, which was collected by suction filtration. If the product was still oily, the supernatant liquid was decanted and the ethanol wash and ether precipitation were repeated. An alternative method involved addition of 25 mL of ether to the flask containing the oil, following by scraping of the oil with a spatula until it dried to a powder.)

Crystalline material was obtained by dissolving the crude product in 3–4 mL of hot CH_3CN followed by gravity filtration of the hot solution into a 20-mL screw-cap vial. The solution volume was decreased by boiling the solution until the product began to precipitate. The vial was then sealed and heated until the solution boiled and the product redissolved. The vial was then allowed to cool slowly to room temperature and was stored at −28 °C overnight to complete crystallization. The crystals were collected by suction filtration, washed with 25 mL of ether, and dried in vacuo to yield 2.3 g (1.1 mmol, 40% yield based on W) of white powder. At this point the product is quite pure and suitable for use in subsequent reactions. The ^{17}O NMR spectrum of this product,

(4) Flynn, C. M., Jr.; Stucky, G. D. *Inorg. Chem.* **1969**, *8*, 178–180.
(5) Johnson, G. K.; Murmann, R. K. *Inorg. Synth.* **1979**, *19*, 140–145.
(6) Che, T. M.; Day, V. W.; Francesconi, L. C.; Fredrich, M. F.; Klemperer, W. G.; Shum, W., submitted for publication in *Inorg. Chem.*
(7) Perrin, D. D.; Armarego, W. L. F.; Perrin, D. R. "Purification of Laboratory Chemicals", 2nd ed.; Pergamon Press: New York, 1980; pp 249–250.

(8) The $TaW_5O_{19}^{3-}$ ion is reported here for the first time. On the basis of analytical as well as IR and ^{17}O NMR spectroscopic data, it is assumed to be isostructural with $NbW_5O_{19}^{3-}$ (see Figure 3 or 4).

Table I. Properties of Selected Magnetic Nuclei

nuclide[a]	natural abundance, %	spin	quadrupole moment, b
^{183}W	14.40	1/2	0[b]
^{97}Mo	9.46	5/2	1.1[b]
^{95}Mo	15.72	5/2	0.12[b]
^{181}Ta	99.99	7/2	3[b]
^{93}Nb	100	9/2	−0.2[b]
^{51}V	99.76	7/2	−0.05[c]

[a] All naturally occurring spins >0 are listed for W, Mo, Ta, Nb, and V. [b] Lee, K.; Anderson, W. A. In "CRC Handbook of Chemistry and Physics", 62nd ed.; Weast, R. C., Astle, J. A., Eds.; CRC Press: Boca Raton, FL, 1981; pp E67-E69. [c] Childs, W. J. *Phys. Rev.* 1967, *156*, 71-82.

however, shows several small impurities (<5%).

To obtain spectroscopically pure product, a different crystallization method was used. In this method, the crude product was dissolved in 3–4 mL of hot CH_3CN and filtered into a 20-mL screw-cap vial. Ether was then added until the product began to precipitate. The vial was then sealed and carefully heated until the product dissolved. Slow cooling to room temperature followed by storage overnight at −28 °C afforded ca. 0.8 g of clear rod-shaped crystals, which were suction filtered, washed with 25 mL of ether, and then dried in vacuo. Crystallization yields varied from 30 to 40%.

The analytical sample was crystallized three times from CH_3CN; the ^{17}O NMR sample was crystallized once from CH_3CN/ether. Anal. Calcd for $C_{48}H_{108}N_3TaW_5O_{19}$: C, 27.05; H, 5.11; N, 1.97; Ta, 8.49; W, 43.13. Found: C, 27.14; H, 5.13; N, 1.99; Ta, 8.46; W, 42.97. IR (Nujol, 700–1000 cm^{-1}, see Figure 2a): 735 (m), 805 (s, br), 884 (m), 907 (m), 957 (s), 975 (sh) cm^{-1}. This preparation has been scaled up by a factor of 3 without complication. According to ^{17}O NMR spectroscopy, the product enrichment is nonstatistical, with the unique OTa oxygen site having low ^{17}O content.

$NbW_5O_{19}[(n\text{-}C_4H_9)_4N]_3$.[9] This compound was prepared with use of the procedure described for $TaW_5O_{19}[(n\text{-}C_4H_9)_4N]_3$ by substituting 2.18 g (6.85 mmol) of $Nb(OC_2H_5)_5$ for $Ta(OC_2H_5)_5$. The yields of both products are comparable. The analytical sample was crystallized three times from CH_3CN; the ^{17}O NMR sample was crystallized once from CH_3CN/ether. As is the case for the tantalum compound (see above), the preparation may be scaled up, and ^{17}O enrichment is low at the ONb site. Anal. Calcd for $C_{48}H_{108}N_3NbW_5O_{19}$: C, 28.21; H, 5.33; N, 2.06. Found: C, 28.10; H, 5.17; N, 2.04. IR[9] (Nujol, 700–1000 cm^{-1}, see Figure 2b): 733 (m), 802 (s, br), 884 (m), 913 (m), 957 (s), 974 (sh) cm^{-1}.

Aqueous $Na_6V_{10}O_{28}$. A 20-mL screw-cap vial was charged with 0.754 g (0.53 mmol) of $Na_6V_{10}O_{28}\cdot 18H_2O$, a stir bar, and 2.65 mL of deionized water. To this solution was added 0.345 mL of 20 atom % ^{17}O water. The vial was capped and immersed to the level of the liquid in an oil bath equilibrated at 40–45 °C. The contents of the vial were stirred overnight, cooled to room temperature, and transferred to a 12-mm sample tube.

Background

When one considers the effect of metal–oxygen spin–spin coupling on ^{17}O NMR line widths, several properties of the metal nuclei in question must be taken into account (see Table I). Clearly, magnetic metal nuclei must have substantial natural abundance to significantly broaden the observed ^{17}O NMR line widths. The spin I of the metal nucleus also plays a key role, affecting ^{17}O NMR line widths in two ways. First, large line widths result from large I values since spin–spin coupling yields $2I + 1$ components in the ^{17}O NMR multiplet for an oxygen bound to a single metal nucleus and yet more components for an oxygen bonded to more than one metal. Second, the metal nucleus' quadrupolar relaxation rate depends on its spin value:

$$\frac{1}{T_1} = \frac{3}{40}\left[\frac{2I+3}{I^2(2I-1)}\right]\left(1+\frac{\eta^2}{3}\right)\left(\frac{e^2qQ}{\hbar}\right)^2\tau_c \qquad (1)$$

In eq 1, which holds under conditions of rapid, isotropic molecular tumbling in a homogeneous medium,[10] η is the electric field gradient asymmetry parameter, q is the largest component of the electric field gradient, e is the charge on the electron, Q is the nuclear electric quadrupole moment, and τ_c is the correlation time for molecular rotation. Thus, smaller I values for a given metal lead to narrower ^{17}O line widths when $I > 1/2$ since small I values imply fast quadrupolar relaxation and fast metal nucleus relaxation serves to decouple the metal spins from the oxygen spins. Equation 1 similarly shows the effect of the metal nucleus' quadrupole moment Q on ^{17}O NMR line width: large Q values imply fast metal quadrupole relaxation and consequently greater metal decoupling. Note finally that the magnitudes of metal–oxygen spin–spin coupling constants also influence the magnitude of spin–spin coupling effects. Unfortunately, very few relevant values have been reported: $|^1J(^{183}W,^{17}O)| < 10$ Hz in WO_4^{2-},[11] $|^1J(^{95}Mo,^{17}O)| = 40$ Hz in MoO_4^{2-},[12] and $|^1J(^{51}V,^{17}O)| = 62$ Hz in VO_4^{3-}.[13]

The effects of metal–oxygen coupling on ^{17}O NMR line widths in polyoxoanions follow a pattern consistent with the properties given in Table I. Neither tungsten- nor molybdenum–oxygen coupling contributes significantly to the line widths at half-height of oxygen resonances in polyoxoanions,[1] a result that follows from (1) low natural abundances of ^{183}W, ^{97}Mo, and ^{95}Mo, (2) the low spin of ^{183}W, (3) small values of $^1J(^{183}W,^{17}O)$, and (4) the large quadrupole moment of ^{97}Mo that leads to rapid quadrupolar relaxation and consequently ^{97}Mo decoupling. The spin $7/2$ ^{181}Ta nucleus is 99.99% abundant but has a quadrupole moment even greater than that of ^{97}Mo. Given that ^{97}Mo is decoupled from ^{17}O in MoO_4^{2-},[12] where molybdenum is in a symmetric environment and quadrupole relaxation is relatively slow, decoupling of ^{181}Ta from ^{17}O in less symmetric polyoxoanions is to be expected. It is therefore not surprising to see no substantial ^{181}Ta–^{17}O coupling effects in the ^{17}O NMR spectrum of $TaW_5O_{19}^{3-}$ (see Table II). Metal relaxation is slower, however, in the cases of ^{93}Nb and ^{51}V, which have smaller quadrupole moments, and the ^{17}O NMR resonances for oxygens bonded to these metals in $NbW_5O_{19}^{3-}$ and $VW_5O_{19}^{3-}$ are severely broadened by oxygen–metal coupling (see Table II and ref 1, respectively).

In light of the above considerations, the problem of improving ^{17}O NMR spectral resolution for early-transition-metal polyoxoanions through metal decoupling reduces to the problem of ^{93}Nb and ^{51}V decoupling. A potentially simple solution to this problem is the thermal-decoupling technique, which has been widely used to decouple quadrupolar nuclei from spin $1/2$ nuclei, for example, ^{14}N from ^1H,[3a] ^{14}N from ^{19}F,[3b] and ^{11}B from ^1H.[3c] This approach takes advantage of the fact that rapid quadrupolar relaxation yields spin–spin decoupling, the quadrupolar relaxation rate is directly proportional to the correlation time for molecular rotation (τ_c in eq 1), and this correlation time usually increases as sample temperature is lowered and sample viscosity is raised.[1,14] Reducing sample temperature thus decouples the quadrupolar nucleus. This approach is unfortunately of limited usefulness in ^{17}O NMR spectroscopy, because the ^{17}O nucleus itself is quadrupolar and relaxes more rapidly at lower temperatures. Line narrowing obtained from thermal decoupling may therefore be offset by increased oxygen quadrupolar broadening. The temperature dependences of ^{17}O NMR line widths for $NbW_5O_{19}^{3-}$ shown in Figure 3 clearly illustrate the competition between thermal ^{93}Nb decoupling and ^{17}O quadrupolar broadening: (1) In the OW and OW_2 regions, where ^{93}Nb coupling is negligible, ^{17}O quadrupolar broadening dominates line width and highest resolution is obtained at high temperature. (2) The ONbW resonance's line width is narrowed by thermal decoupling but only by lowering the temperature to the point where rapid ^{17}O quadrupolar relaxation significantly broadens all ^{17}O resonances. (3)

(9) An alternative route to this compound, unsuitable for the preparation of ^{17}O-enriched material, has been reported recently: Sanchez, C.; Livage, J.; Launay, J. P.; Fournier, M. *J. Am. Chem. Soc.* **1983**, *105*, 6817–6823.

(10) Abragam, A. "The Principles of Nuclear Magnetism"; Oxford University Press: London: 1961; p 314.
(11) Banck, J.; Schwenk, A. *Z. Phys. B* **1975**, *20*, 75–80.
(12) Vold, R. R.; Vold, R. L. *J. Chem. Phys.* **1974**, *61*, 4360–4361.
(13) Lutz, O.; Nepple, W.; Nolle, A. *Z. Naturforsch., A* **1976**, *31A*, 1046–1050.
(14) In ref 10, p 300.

Table II. 33.9-MHz ^{17}O and $^{17}O\{^{93}Nb\}$ NMR Spectral Data for $TaW_5O_{19}^{3-}$, $NbW_5O_{19}^{3-}$, and *cis*-$Nb_2W_4O_{19}^{4-}$ [a]

anion and temp, °C	^{93}Nb decoupled	chemical shifts[b,c] (line widths[d])					
		OM	OW	OM_2	OMW	OW_2	$O(M/W)_6$
$TaW_5O_{19}^{3-}$		666	733, 731[e]		420	394, 393	−73
80	no	(95)	(54)[f]		(42)	(73)[f]	(14)
$NbW_5O_{19}^{3-}$		799	732, 730		456	394, 392	−67
75	no	[g]	(47)[f]		(790)	(42)[f]	(16)
28	no	[g]	(73)[f]		(710)	(102)[f]	(16)
28	yes	(88)	(62)[f]		(23)	(99)[f]	(16)
0	no	[g]	(109)[h]		(590)	(110)[f]	(21)
−18	no	[g]	(152)[h]		(448)	(120)[h]	(25)
$Nb_2W_4O_{19}^{4-}$		753	691[h]	493	435[h]	374[h]	
52	no	(243)	(82)	(145)	(92)	(90)	
52	yes	(147)	(81)	(54)	(60)	(85)	
−16	no	(333)	(213)	(91)	(97)	(199)	

[a] See Experimental Section for experimental parameters. [b] An oxygen environment is identified by the number and type of metal atoms an oxygen is bonded to. The symbol M represents Nb or Ta. Resonances were assigned following procedures outlined in ref 1. [c] Chemical shifts given in ppm. No variations in chemical shift values were observed over the temperature ranges given in column 1. [d] Line widths (fwhm, in Hz) are enclosed in parentheses. [e] Shoulder. [f] Combined line width of the resonances listed was measured at the half-height of the most intense resonance. [g] Resonance could not be located. [h] Individual resonances unresolved. [i] Not observed due to insufficient ^{17}O content. See ref 2.

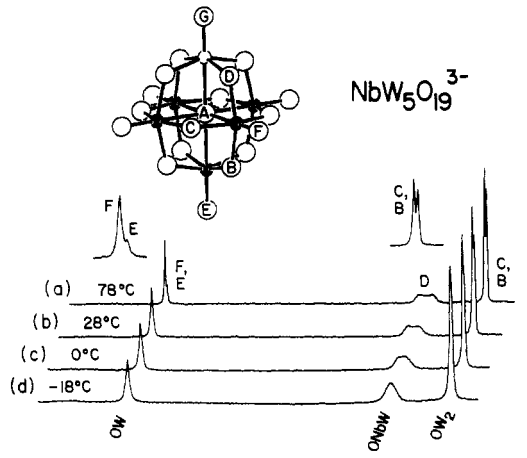

Figure 3. (Top) SCHAKAL drawing of the C_{4v} $NbW_5O_{19}^{3-}$ anion. The small filled circles represent tungsten atoms, the small open circle represents the niobium atom, and large open circles represent oxygen atoms. One member of each set of symmetry-equivalent oxygen atoms is labeled. (Bottom) δ 350–825 regions of 33.9-MHz ^{17}O NMR spectra of $(NbW_5O_{19})[(n\text{-}C_4H_9)_4N]_3$ in CH_3CN measured at four different temperatures (a–d). The insets are horizontal expansions of the OW and OW_2 regions at 78 °C. See Table II and the Experimental Section for numerical data and experimental parameters.

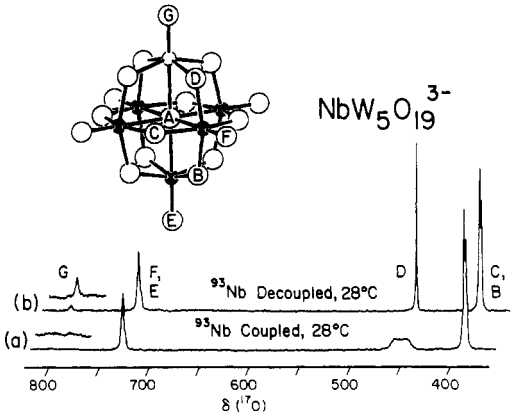

Figure 4. (Top) SCHAKAL drawing of the C_{4v} $NbW_5O_{19}^{3-}$ anion. See the Figure 3 caption for an explanation of the labeling scheme. (Bottom) Niobium-93 coupled (a) and decoupled (b) 33.9-MHz ^{17}O NMR spectra of $(NbW_5O_{19})[(n\text{-}C_4H_9)_4N]_3$ in CH_3CN. In each spectrum, only the δ 350–825 region is shown. The two insets are vertical expansions of the δ 770–825 regions. See Table II for numerical data and the Experimental Section for experimental parameters.

The ONb resonance arising from the oxygen labeled O_G at the top of Figure 3 is too broad to detect at high temperatures because of ^{93}Nb coupling and at low temperatures because of ^{17}O quadrupolar broadening.[15]

Double-Resonance Experiments

$^{17}O\{^{93}Nb\}$ NMR. The spectra of $NbW_5O_{19}^{3-}$ shown in Figure 4 illustrate the effects that metal decoupling can have on ^{17}O NMR line widths: the line width of the 456 ppm ONbW (O_D) resonance narrows by a factor of $^1/_{30}$ upon ^{93}Nb decoupling (see Table II); the 799 ppm O_G resonance, which appears in the decoupled spectrum, is too broad to be observed in the ^{93}Nb-coupled spectrum. The effect of metal decoupling is not so dramatic in other cases where the metal quadrupole relaxation rate is more rapid. The $Nb_2W_4O_{19}^{4-}$ ion, for example, has a ^{93}Nb NMR line that is about 8 times as broad as the ^{93}Nb NMR line for $NbW_5O_{19}^{3-}$ (see Table III), indicating a ^{93}Nb quadrupolar relaxation rate about 8 times as fast. This more rapid relaxation rate has four consequences (see Table II and Figure 5): (1) The ONb and ONbW ^{17}O resonances from $Nb_2W_4O_{19}^{4-}$ are not as severely broadened by ^{93}Nb coupling as the corresponding $NbW_5O_{19}^{3-}$ resonances (Figure 5b). (2) Thermal decoupling is observed only for the ONb_2 resonance, and the ONb and ONbW resonances actually broaden upon lowering the temperature from 51 to −16 °C (see Figure 5c). (3) The effect of ^{93}Nb decoupling upon ONb and ONbW ^{17}O NMR line widths is less pronounced in the $Nb_2W_4O_{19}^{4-}$ case than in the $NbW_5O_{19}^{3-}$ case. (4) Con-

Table III. 61.1-MHz ^{93}Nb NMR Spectral Data for $NbW_5O_{19}^{3-}$ and *cis*-$Nb_2W_4O_{19}^{4-}$ [a]

anion	chem shift[b]	temp, °C	line width[c]
$NbW_5O_{19}^{3-}$	−888	75	500
		28	670
		0	800
		−18	950
$Nb_2W_4O_{19}^{4-}$	−890	52	4300
		21	5700
		−16	7000

[a] See Experimental Section for experimental parameters. [b] Chemical shifts given in ppm. No variations in chemical shift values were observed over the temperature ranges given in column 3. [c] Line widths are fwhm, in Hz.

(15) Addition of ^{17}O-enriched water to $NbW_5O_{19}[(n\text{-}C_4H_9)_4N]_3$ in acetonitrile results in selective enrichment of the ONb oxygen. In this fashion, large amounts of compound highly enriched in ^{17}O at the ONb site can be prepared economically. A 0.1 M solution of compound enriched to 36% ^{17}O displays an 800 ppm ONb resonance with a >1 KHz line width at 25 °C.

Table IV. 33.9-MHz ^{17}O and $^{17}O\{^{51}V\}$ NMR Spectral Data for Aqueous $Na_6V_{10}O_{28}$[a]

temp, °C	^{51}V resonance decoupled[b]	chemical shifts[c,d] (line widths[e])							
		O_G	O_F	metavanadates	O_E	O_D	O_C	O_B	O_A
44		1152	1142	923	897	795	761	391	66
	...	(750)[f]		(>1000)	(220)	(305)	(299)	(274)	(43)
	i	(754)[f]		(>1000)	(83)	(292)	(292)	(246)	(37)
	ii	(86)	(305)	(>1000)	(198)	(83)	(208)	(246)	(38)
	iii	(235)	(110)	(>1000)	(206)	(204)	(143)	(222)	(37)
	iv	(757)[f]		(>1000)	(218)	(288)	(295)	(278)	(42)
19		1151	1138	929, 473	897	789	765	400	62
	...	(760)[f]		(495, >1000)	(170)	(282)	(282)	(300)	(64)
	iv	(770)[f]		(308, 630)	(175)	(280)	(280)	(295)	(64)

[a] See Experimental Section for experimental parameters. [b] ^{51}V resonances labeled as follows: δ −422, i; δ −497, ii; δ −512, iii; δ −576, iv. See Figure 7. [c] Assignments are made in ref 17 and in the text. See Figure 6 and 7 for $V_{10}O_{28}^{6-}$ oxygen-labeling scheme. [d] Chemical shifts given in ppm. [e] Line widths (fwhm, in Hz) enclosed in parentheses. [f] Combined line width of O_F and O_G resonances, measured at the half-height of the more intense resonance.

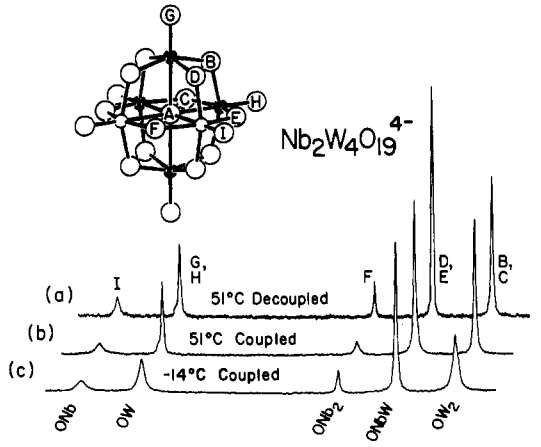

Figure 5. (Top) SCHAKAL drawing of the C_{2v} *cis*-$Nb_2W_4O_{19}^{4-}$ anion. See the Figure 3 caption for an explanation of the labeling scheme. (Bottom) Niobium-93 decoupled (a) and coupled (b) 33.9-MHz ^{17}O NMR spectra of $(Nb_2W_4O_{19})[(n\text{-}C_4H_9)_4N]_4$ in CH_3CN at 51 °C. The ^{93}Nb-coupled ^{17}O NMR spectrum shown in (c) was measured at −14 °C. In each spectrum, only the δ 375–800 region is shown. See Table II for numerical data and the Experimental Section for experimental parameters.

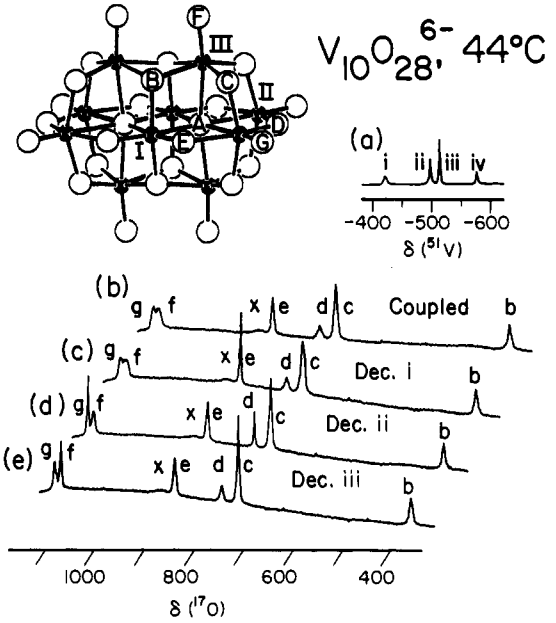

Figure 6. (Top) SCHAKAL drawing of the D_{2h} $V_{10}O_{28}^{6-}$ anion. Small filled circles represent vanadium atoms, and large open circles represent oxygen atoms. One member from each set of symmetry-equivalent oxygen and vanadium atoms is labeled. (Bottom) 65.8-MHz ^{51}V NMR spectra and 33.9-MHz ^{17}O and $^{17}O\{^{51}V\}$ NMR spectra (a–e), all measured from an aqueous $Na_6V_{10}O_{28}$ solution at 44 °C. Only the δ 325–1200 region is shown in (b–e). See Tables IV and V for numerical data and the Experimental Section for experimental parameters.

siderably more decoupling power is needed to perform the $^{17}O\{^{93}Nb\}$ NMR experiment for $Nb_2W_4O_{19}^{4-}$ (ca. 22 W) than for $NbW_5O_{19}^{3-}$ (ca. 10 W) since the effective frequency range of the decoupling field must be increased considerably. In short, when an ^{17}O NMR spectrum is substantially decoupled from ^{93}Nb thermally, double-resonance experiments require more decoupling power to achieve less decoupling.

$^{17}O\{^{51}V\}$ NMR. The $V_{10}O_{28}^{6-}$ ion contains three structurally nonequivalent vanadium sites (see Figure 6) and thus provides an opportunity for investigating the effectiveness of selective metal decoupling. The ^{51}V NMR spectrum of aqueous $Na_6V_{10}O_{28}$ contains three resonances, labeled i–iii in Figure 6a, which arise from the $V_{10}O_{28}^{6-}$ ion and a single resonance, labeled iv in Figure 6a, which arises from one or more cyclic metavanadate ions $(VO_3)_n^{n-}$.[16] Resonance i can be assigned to V_I in the $V_{10}O_{28}^{6-}$ structure with use of intensity arguments. Resonances ii and iii are assigned to V_{II} and V_{III}, but a unique assignment for each of these two resonances is not possible since they have equal intensities. The ^{17}O NMR spectrum of aqueous $Na_6V_{10}O_{28}$ also contains resonances for both $V_{10}O_{28}^{6-}$ and $(VO_3)_n^{n-}$[16f,17] (see Figure 6b and Table IV). Although metavanadates should display both terminal and bridging oxygens, only a single broad resonance, labeled x in Figure 6, appears in the region expected for dioxo terminal oxygens. The seven remaining ^{17}O resonances are assigned to the $V_{10}O_{28}^{6-}$ anion:[17] resonances a–e are assigned to oxygens O_A–O_E, respectively; resonances f and g correspond to oxygens O_F and O_G, but unique assignments of these two resonances is not possible.

A complete, unique assignment of all ^{51}V and ^{17}O NMR resonances for the $V_{10}O_{28}^{6-}$ anion can be obtained from the set of three selectively decoupled $^{17}O\{^{51}V\}$ spectra shown in Figure 6c–e. Decoupling of ^{51}V resonance i, already assigned to V_I, narrows only the O_E resonance e. Although V_I is also bonded to O_A and O_B, resonances a and b are not narrowed because they are still coupled to two or more V_{II} and/or V_{III} centers. The most pronounced effects of decoupling ^{51}V resonance ii are the narrowing of ^{17}O resonances d and g. Since resonance d is assigned to O_D, and O_D is bonded to V_{II} only, ^{51}V resonance ii is assigned to V_{II} and ^{17}O resonance g is assigned to O_G. This scheme implies assignments of ^{51}V resonance iii to V_{III} and ^{17}O resonance f to O_F; decoupling of ^{51}V resonance iii confirms these assignments. Closer examination of ^{17}O line widths in Figure 6d,e shows the

(16) (a) Hatton, J. V.; Saito, Y.; Schneider, W. G. *Can. J. Chem.* **1965**, *43*, 47–56. (b) Howarth, O. W.; Richards, R. E. *J. Chem. Soc.* **1965**, 864–870. (c) Kazanskii, L. P.; Spitsyn, V. I. *Dokl. Akad. Nauk SSSR* **1975**, *223*, 381–384. (d) O'Donnell, S. E.; Pope, M. T. *J. Chem. Soc., Dalton Trans.* **1976**, 2290–2297. (e) Habayeb, M. A.; Hileman, O. E., Jr. *Can. J. Chem.* **1980**, *58*, 2255–2261. (f) Heath, E.; Howarth, O. W. *J. Chem. Soc., Dalton Trans.* **1981**, 1105–1110. (g) Petterson, L.; Hedman, B.; Andersson, I.; Ingri, N. *Chem. Scr.* **1983**, *22*, 254–264.
(17) Klemperer, W. G.; Shum, W. *J. Am. Chem. Soc.* **1977**, *99*, 3544–3545.

Table V. 65.8-MHz ^{51}V NMR Spectra Data for Aqueous $Na_6V_{10}O_{28}$[a]

temp, °C	chemical shifts[b,c] (line widths[d])			
	V_I	V_{II}	V_{III}	metavanadates
44	−422 (355)	−497 (260)	−512 (150)	−576 (220)
35	−422 (410)	−498 (300)	−513 (155)	−576, −582[e] (160)
19	−423 (580)	−498 (430)	−514 (210)	−575, −584 (120, 200)

[a] Spectra are shown in Figure 7a–c. See Experimental Section for experimental parameters. [b] Assignments are made in text. See Figure 6 or 7 for $V_{10}O_{28}^{6-}$ vanadium-labeling scheme. [c] Chemical shifts given in ppm. [d] Line widths (fwhm, in Hz) enclosed in parentheses. [e] Shoulder.

V_{II} and V_{III} ^{51}V decoupling is not completely selective; i.e., decoupling of resonance ii, for example, affects not only the line width of ^{17}O resonance g but also the line width of resonance f to a lesser extent. Although this effect might be attributed to long-range ^{51}V–^{17}O coupling, it is easily shown to arise from off-resonance decoupling by varying the ^{51}V decoupling frequency in the neighborhood of a ^{51}V resonance and observing the effect in ^{17}O NMR line widths.

We were somewhat surprised to observe that decoupling of the metavanadate ^{51}V resonance iv (Figure 6a) has no effect on the line width of the metavanadate ^{17}O resonance x (Figure 6b). Clearly, this ^{17}O NMR line width is not controlled by ^{51}V coupling but instead by either ^{17}O quadrupolar relaxation or chemical-exchange broadening. To investigate this latter possibility, we measured ^{51}V and ^{17}O NMR spectra of $Na_6V_{10}O_{28}$ solutions at lower temperatures. As indicated in Table V, ^{51}V resonances i–iii assigned to $V_{10}O_{28}^{6-}$ broadened as the temperature is lowered, the expected behavior for resonances whose line width is controlled by quadrupolar relaxation rate. The metavanadate resonance iv, however, undergoes line-shape changes characteristic of a system undergoing rapid chemical exchange (see also Figure 7a–c). At 19 °C, two metavanadate resonances are observed, and as the temperature is raised, these lines broaden and coalesce into a single resonance, which narrows as the temperature is further increased. Moreover, the $^{17}O\{^{51}V\}$ NMR spectrum at 19 °C (Figure 7e) shows line narrowing relative to the ^{17}O NMR spectrum at 19 °C (Figure 7d) of both the metavanadate terminal oxygen resonance x and the metavanadate briding oxygen resonance y. This result demonstrates that the line narrowing of metavanadate ^{17}O resonances that accompanies the temperature change from 44 to 19 °C is a consequence of chemical exchange, not thermal decoupling.

Conclusions

1. Of the nonzero-spin early-transition-metal nuclei ^{183}W, ^{97}Mo, ^{95}Mo, ^{181}Ta, ^{93}Nb, and ^{51}V, which can potentially broaden ^{17}O NMR resonances through spin–spin coupling, only ^{93}Nb and ^{51}V are found to substantially influence ^{17}O NMR spectral resolution.

2. Thermal ^{51}V and ^{93}Nb decoupling is in general not a useful method for improving ^{17}O NMR spectral resolution since lower temperatures increase the rate of ^{17}O quadrupolar relaxation and therefore broaden ^{17}O resonances.

3. Double-resonance experiments can dramatically reduce ^{17}O NMR line widths as illustrated by $^{17}O\{^{93}Nb\}$ NMR studies of $NbW_5O_{19}^{3-}$ and $Nb_2W_4O_{19}^{4-}$.

4. Selective metal decoupling is a powerful tool for assigning both metal and oxygen resonances as demonstrated by an $^{17}O\{^{51}V\}$ NMR study of $V_{10}O_{28}^{6-}$.

5. Metal decoupling is an effective aid in the interpretation of variable-temperature ^{17}O NMR spectra, as illustrated by an $^{17}O\{^{51}V\}$ study of aqueous metavanadates $(VO_3)_n^{n-}$, since it allows a separation of oxygen quadrupolar broadening and thermal metal decoupling effects, which both broaden ^{17}O resonances as the temperature is lowered.

6. Although decoupling power levels as high as 22 W are sometimes required, the resulting sample heating can be adequately compensated for with use of standard gas cooling.

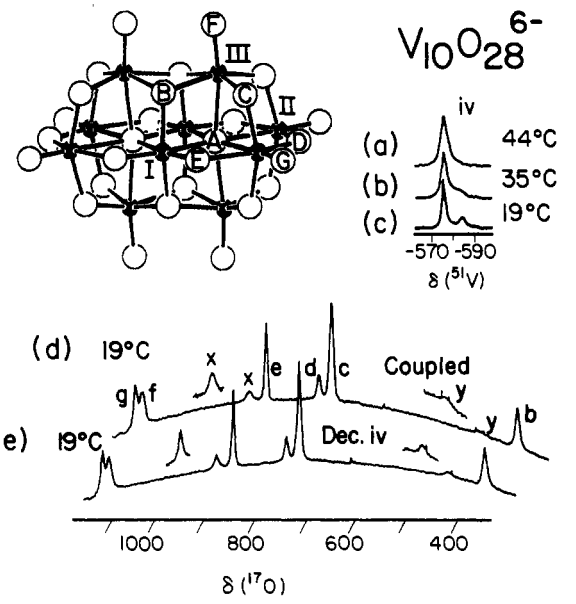

Figure 7. (Top) SCHAKAL drawing, labeled as described in the Figure 6 caption. (Bottom) Temperature-dependent 65.8-MHz ^{51}V NMR spectra of aqueous $Na_6V_{10}O_{28}$ in the δ −550 to −600 (a–c). The 33.9-MHz ^{17}O and $^{17}O\{^{51}V\}$ NMR spectra shown in (d) and (e) were measured from the same sample at 19 °C. The insets in (d) and (e) are vertical expansions of the metavanadate resonances labeled x and y. See Tables IV and V for numerical data and the Experimental Section for experimental parameters.

Acknowledgment. This research was supported by the National Science Foundation. NMR experiments were conducted at the University of Illinois NSF Regional NMR Facility (Grant CHE 97-16100). We are grateful to Denny Warrenfeltz for extensive technical assistance.

Registry No. ^{51}V, 7440-62-2; ^{93}Nb, 7440-03-1; ^{181}Ta, 7440-25-7; ^{95}Mo, 14392-17-7; ^{97}Mo, 14392-19-9; ^{183}W, 14265-81-7; ^{17}O, 13968-48-4; $NbW_5O_{19}^{3-}$, 60098-32-0; $Nb_2W_4O_{19}^{4-}$, 60098-33-1; $V_{10}O_{28}^{6-}$, 12397-12-5; $Na_6V_{10}O_{28}$, 12200-88-3.